Appl. Phys. B 90, 547–556 (2008)
DOI: 10.1007/s00340-007-2886-1

Applied Physics B
Lasers and Optics

LITTY IRIMPAN[1,✉]
A. DEEPTHY[2]
BINDU KRISHNAN[3]
V.P.N. NAMPOORI[1]
P. RADHAKRISHNAN[1]

Nonlinear optical characteristics of self-assembled films of ZnO

[1] International School of Photonics, Cochin University of Science and Technology, Cochin 682022, Kerala, India
[2] Amrita Institute of Medical Sciences, Cochin, India
[3] Centre for Materials for Electronics Technology, Thrissur, India

Received: 3 May 2007/Revised version: 5 November 2007
Published online: 24 January 2008 • © Springer-Verlag 2008

ABSTRACT In the present work, we have investigated the nonlinear optical properties of self-assembled films formed from ZnO colloidal spheres by z-scan technique. The sign of the nonlinear component of refractive index of the material remains the same; however, a switching from reverse saturable absorption to saturable absorption has been observed as the material changes from colloid to self-assembled film. These different nonlinear characteristics can be mainly attributed to ZnO defect states and electronic effects when the colloidal solution is transformed into self-assembled monolayers. We investigated the intensity, wavelength and size dependence of saturable and reverse saturable absorption of ZnO self-assembled films and colloids. Values of the imaginary part of third-order susceptibility are calculated for particles of size in the range 20–300 nm at different intensity levels ranging from 40 to 325 MW/cm^2 within the wavelength range of 450–650 nm.

PACS 81.16.Dn; 42.65.-k; 42.65.An; 42.70.-a; 42.70.Nq; 78.20.Ci

1 Introduction

The search for new nonlinear optical materials with high optical nonlinearities is gaining interest both from the research as well as industrial point of view. The essential requirements of good photonic materials are its large and fast acting nonlinearity, synthetic flexibility and ease of processing. In recent years, wide band gap semiconductors have been subjected to extensive studies because of the rising interest in the development of new nonlinear optical materials for potential applications in integrated optics. Impressive progress has been made in fabricating nonlinear optical waveguides from several nonlinear optical single crystals, which tend to be rather expensive. ZnO is an interesting wurtzitic II–VI wide band gap semiconductor that has a room-temperature band gap of ~ 3.3 eV, combined with high excitonic gain and large excitonic binding energy. The optical properties of this material are currently the subject of tremendous investigations, in response to the industrial demand for optoelectronic devices that could operate at short wavelengths. There is a significant demand for thin film nonlinear optical materials, which can be integrated into an optoelectronic device. Recent studies have revealed that ZnO self-assembled films can act as photonic crystals.

Photonic crystals show a great deal of applications in numerous types of devices in 1, 2, and 3D structures. Due to its promising applications such as integrated optical circuits and thresholdless lasers, photonic crystals have been intensively investigated [1]. Numerous techniques have been devised in an effort to produce periodic arrays of dielectric materials that can exhibit a photonic stop band. The fabrication of photonic crystals that work in the visible or near-infrared range is still a challenging topic. The principal method involves semiconductor fabrication technology, which includes lithography, layering, and etching processes. Several sophisticated methods have been developed such as laser microfabrication, but they require expensive and large scale equipment [2]. One of the simplest techniques of fabricating photonic crystals involves colloidal self-assembly, wherein, monodisperse colloidal spheres will spontaneously assemble into periodic arrays under certain circumstances. Zinc oxide is a promising candidate for optically active self-assembled photonic crystals [3].

Most of the work performed in the area of self-assembled 3D photonic crystals has involved a few materials which are readily available as monodisperse colloidal spheres in sizes appropriate for photonic crystals including SiO_2 and polymers, such as polystyrene and PMMA [4]. In addition, while some studies have been performed in which emissive materials are added to the photonic crystal matrix [5], no work has explored the properties of photonic crystals formed directly from optically active materials. Van Blaaderen et al. have produced a number of interesting emissive materials as monodisperse colloidal spheres, including Er^{3+} doped SiO_2, dye-doped PMMA, and SiO_2/ZnS core/shell structures [6]. ZnO is a promising candidate for optically active self-assembled photonic crystals because of its higher refractive index (2.1–2.2 in the visible regime) compared to other materials (1.4–1.5 for SiO_2 and most polymers). In addition, ZnO has been found to be an efficient emitter, exhibiting lasing behavior in the near UV region ($\lambda \approx 385$ nm) [7].

Accordingly, designing novel ZnO material and, in particular, well-defined anisotropic and highly oriented 3D large arrays is of great importance for basic fundamental research

✉ Fax: +91-484-2576714, E-mail: littyirimpan@yahoo.co.in

as well as of relevance for various fields of industrial and high technology applications. The thermodynamically stable crystallographic phase of this polar non-transition metal oxide is wurtzite and occurs in nature as the mineral zincite (although scarcely as natural single crystal). ZnO has a hexagonal lattice, with an $a : c$ axial ratio of 1 : 1.6 [8]. Its ionic and polar structure can be described as a hexagonal close packing (HCP) of oxygen and zinc atoms in point group $3m$ and space group $P63mc$ with zinc atoms in tetrahedral sites. The occupancy of four of the eight tetrahedral sites of HCP arrays controls the structure. The hexagonal unit cell contains two formula units, and the crystal habit exhibits a basal polar plane ($001h$) and two types of low-index faces, a nonpolar ($1h00$) face (and $C6V$ symmetric ones) and a tetrahedron corner-exposed polar (001) face. The "low-symmetry" nonpolar faces with three-fold coordinated atoms are the most stable ones. Additionally, there is no center of inversion in the wurtzite structure; therefore, an inherent asymmetry along the c-axis is present allowing the growth of anisotropic crystallites [9].

An intense radiation can induce a profound change on the absorption property of a material, resulting in the intensity dependent transmittance, which is the so called nonlinear absorption [10]. Nonlinear absorption can be classified into two types: (i) transmittance increases with increasing optical intensity; this case corresponds to the well known saturable absorption (SA); (ii) transmittance reduces with increasing optical intensity; this type includes two photon absorption, multiphoton absorption, and reverse saturable absorption (RSA). Different effects originating from different physical mechanisms can lead to a variety of different applications. For instance, SA materials have been used extensively in short-pulsed laser generations [11] as crucial passive mode-locking or Q-switching elements. Thus, it is paramount to fully characterize saturable performance, in which a typical figure of merit is the saturable intensity. SA characteristics depend on the inherent properties of a material and the parameters such as wavelength, intensity, and pulse duration of the laser used. To characterize nonlinear absorption, the open aperture (OA) z-scan technique, which was first pioneered by Sheik-Bahae et al. [12], has been extensively used. Recently, an OA z-scan theory for the materials with simultaneous two and three-photon absorption has developed, which allows us to identify and determine the two and three photon absorption coefficients from a single OA z-scan trace [13]. The SA properties of some materials are observed experimentally and analyzed theoretically [14]. The theory allows a straightforward estimation of the saturable intensity and the determination of the SA model for a material by fitting the experimental data. We also discuss the possible mechanisms of SA. When the experiment on the characterization of the saturable absorption is performed by using the pulsed laser, if the nonlinear response time of the samples is much shorter than the laser pulse width, one can assume that the nonlinear effect depends on the instantaneous intensity inside the sample.

The studies on nonlinear processes in photonic materials are significant in the context of their technological applications, especially in areas such as passive optical power limiting, optical switching, and the design of logic gates. However, the switching to saturable absorption in ZnO self-assembled films from reverse saturable absorption in colloids have not been explored and reported yet. In this paper, we report our investigations on the size, intensity and wavelength dependence of saturable and reverse saturable absorption of ZnO self-assembled films and colloids using 10 Hz, 5–7 ns pulses from a tunable laser by z-scan method. Values of the imaginary part of third-order susceptibility are calculated for particles of size in the range 20–300 nm at different intensity levels ranging from 40 to 325 MW/cm^2 within the wavelength range of 450–650 nm.

2 Experiment

Colloids of ZnO are synthesized by a modified polyol precipitation method [3]. The monodisperse ZnO colloidal spheres are produced by a two-stage reaction process. The method of preparation involves the hydrolysis of zinc acetate dihydrate (ZnAc; Merck) in diethylene glycol medium (DEG; Merck). Among the different polyols, diethylene glycol (DEG) is chosen because it is reported to give powders with uniform shape and size distribution. The size of the particles and hence the stability of this colloidal suspension depend on the concentration of zinc acetate as well as on the rate of heating. The molar concentration of precursor solution is varied from 0.1 M to 0.5 M and a heating rate of 4 °C per minute is employed for the formation of ZnO at a temperature of 120 °C. The product from the primary reaction is placed in a centrifuge and the supernatant (DEG, dissolved reaction products, and unreacted ZnAc and water) is decanted off and saved. A secondary reaction is then performed to produce the monodisperse ZnO spheres. Prior to reaching the working temperature, typically at 115 °C, some volume of the primary reaction supernatant is added to the solution. After reaching 120 °C, it is stirred for one hour, to get a monodisperse stable colloid. Films are then produced from the ZnO colloidal spheres using a sedimentation self assembly process by the technique of drop casting onto a preheated glass substrate maintained at a temperature of 120 °C.

The ZnO colloids and self-assembled films are characterized by optical absorption measurements recorded using a spectrophotometer (JascoV-570 UV/VIS/IR) and the fluorescence emission measurements recorded using Cary Eclipse fluorescence spectrophotometer (VARIAN). The structural properties of the samples are investigated by X-ray diffraction (XRD) with Ni-filtered Cu K_α (1.5406 Å) source.

When a high irradiance laser beam propagates through any nonlinear material, photoinduced refractive index variations may lead to self-focusing of the beam. The propagation of laser beam inside such a material and the ensuing self refraction can be studied using the z-scan technique. The details of this technique are well documented in literature [15]. It enables one to determine the nonlinear properties of solids, ordinary liquids, and liquid crystals. In this method the intensity dependence of refractive index and absorption are manifested as a position dependent transmission variation of the material, which in turn can be made use of in extracting various nonlinear optical parameters such as real and imaginary parts of susceptibility, cross-sections of nonlinear absorption and nonlinear refraction, etc. However, we are mainly focusing on the particle size, intensity and wavelength dependence of nonlin-

ear absorption studies in ZnO colloid and self-assembled film with particular emphasis on the RSA and SA properties.

In the present investigation, we have employed the single beam z-scan technique with nanosecond laser pulses to measure nonlinear optical absorption and refraction properties of ZnO nano colloids as well as self-assembled spheres. Z-scan technique developed by Sheik Bahae and his coworkers is a single beam method for measuring the sign and magnitude of nonlinear refractive index, n_2, and has sensitivity comparable to interferometric methods [12, 15]. The size dependence and intensity dependence of the samples are investigated using a Q-switched Nd:YAG laser (Spectra Physics LAB-1760, 532 nm, 7 ns, 10 Hz) and the wavelength dependence of the samples are carried out using a tunable laser (Quanta Ray MOPO, 5 ns, 10 Hz). The sample is moved in the direction of light incidence near the focal spot of the lens with a focal length of 200 mm. The radius of the beam waist ω_0 is calculated to be 35.4 μm. The Rayleigh length, $z_0 = \frac{\pi w_0^2}{\lambda}$ is estimated to be 7.4 mm, much greater than the thickness of either the sample cuvette (1 mm) or the self-assembled films, which is an essential prerequisite for z-scan experiments. The transmitted beam energy, reference beam energy and their ratio are measured simultaneously by an energy ratiometer (Rj7620, Laser Probe Corp.) having two identical pyroelectric detector heads (Rjp735). The linear transmittance of the far field aperture S, defined as the ratio of the pulse energy passing the aperture to the total energy is measured to be approximately 0.21. The z-scan system is calibrated using CS_2 as a standard. The effect of fluctuations of laser power is eliminated by dividing the transmitted power by the power obtained at the reference detector. The data are analyzed by using the procedure described by Sheik Bahae et. al and the nonlinear coefficients are obtained by fitting the experimental z-scan plot with the theoretical plots.

3 Results and discussion

Figure 1 gives the room temperature absorption spectra of the ZnO colloid and self-assembled film of size 20 nm. The excitonic peak of the colloid is found to be blue shifted from that of bulk ZnO, which could be attributed to the confinement effects [16]. The breadth of the absorption edge of the self-assembly film indicates that there exists defect-related transitions.

The direct bandgap of ZnO colloids are estimated from the graph of $h\nu$ vs. $(\alpha h\nu)^2$ for the absorption coefficient α that is related to the bandgap E_g as $(\alpha h\upsilon)^2 = k(h\upsilon - E_g)$, where $h\nu$ is the incident light energy and k is the constant. Extrapolation of the linear part until it intersects the $h\nu$ axis gives E_g. The optical band gap (E_g) is found to be shifted from that of the bulk as shown in the inset of Fig. 1. The total change in the band gap of the material is simultaneously contributed by shifts of the valence and the conduction band edges away from each other [17]. In general, the shift of the top of the valence band (TVB) is not the same as that of the bottom of the conduction band (BCB). A larger shift for the BCB is indeed expected in view of the fact that the band-edge shifts are related inversely to the corresponding effective masses and the effective mass of the electron is always much smaller than that of the hole in these II–VI semiconductors. From Fig. 1, it is

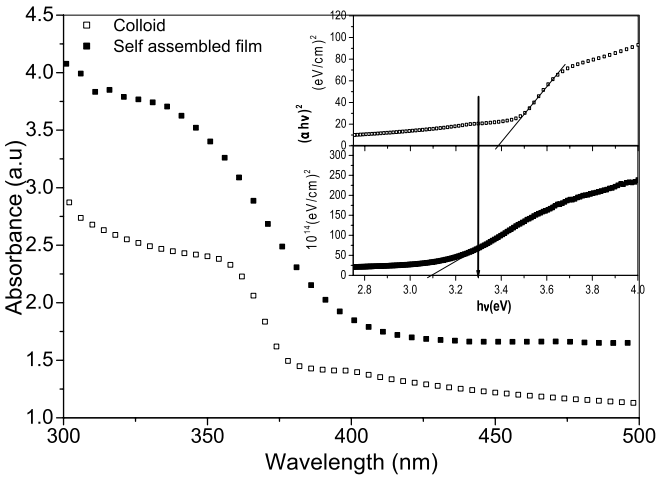

FIGURE 1 Absorption spectra of the ZnO colloid and self-assembled film. The corresponding optical band gaps are shown in the *inset*

clear that the band gap of self-assembled film is reduced to 3.1 eV from that of bulk (3.3 eV) where as the band gap energy of the colloid is higher than that of bulk.

Figure 2 shows the fluorescence spectra of ZnO colloid and self-assembled film of size 20 nm for an excitation wavelength of 325 nm. From the figure it is clear that two emission bands are present, a UV emission band and another in the green region. The UV band has been assigned to the band gap fluorescence and the visible band is mainly due to surface states.

The self-assembled film and powder extracted from the colloid are characterized by X-ray diffraction. Typical XRD patterns of powder extracted from ZnO colloid and self-assembled film are given in Fig. 3a and b respectively. The diffraction pattern and interplane spacings can be well matched to the standard diffraction pattern of wurtzite ZnO, demonstrating the formation of wurtzite ZnO nanocrystals. The particle diameter d is calculated using the Debye–Scherer formula $d = \frac{0.89\lambda}{\beta \cos\theta}$ where λ is the X-ray wavelength (~ 1.5406 Å), θ is the Bragg diffraction angle, and β is the

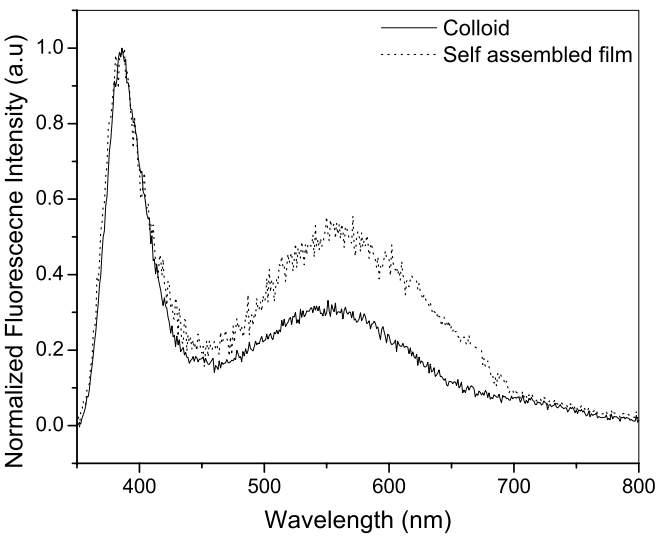

FIGURE 2 Fluorescence spectra of ZnO colloid and self-assembled film for an excitation wavelength of 325 nm

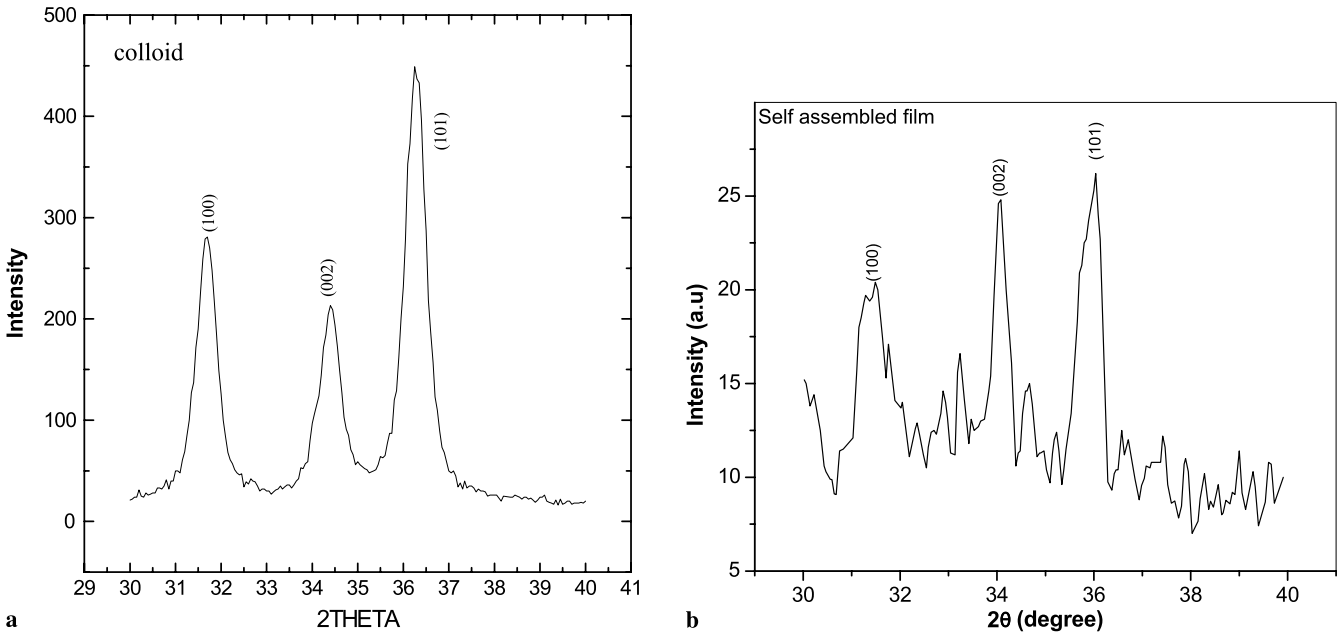

FIGURE 3 (**a**) XRD pattern of the powder extracted from ZnO colloid; (**b**) XRD pattern of ZnO self-assembled film

peak width at half maximum [18]. The XRD peak at 36° in Fig. 3 gives the ZnO particle diameter of 18 and 20 nm, respectively, for the colloid and film, respectively.

Both colloid and film show three major orientations, viz., (100), (002) and (101). The (101) orientation is reported to be the prominent peak having the lowest surface energy and other orientations require more thermal energy to develop. The (002) direction is not the direction of fastest growth for ZnO. This we infer from the fact that the (002) faces of ZnO are the ones with the highest surface energy and these faces, according to basic crystal growth theory should, therefore, be among the faces of lowest growth rate [19]. But the relative intensity for the (002) orientation in self-assembled film is observed to be higher compared to the colloidal spheres. In lattice mismatched epitaxial growth, it is well known that the increase of the length of c-axis causes the decrease of the length of a-axis. This means that ZnO thin film has a tensile built-in strain and the tensile strain in ZnO can be relaxed by providing sufficient thermal energy [19].

The (002) peak is observed at a diffraction angle (2θ) of 34.45° in the powder extracted from colloid and its line width is about 0.60. The diffraction angle from the (002) plane of bulk ZnO powder is 34.4° and its line width is 0.20 [20]. On the other hand, the diffraction angle from the (002) plane of self-assembled film is 34.06° and its linewidth is 0.80. Thus for self-assembled films, a shift of the (002) diffraction angle towards lower angles and an increase in linewidth are also observed. Considering all these observations and the reduction of band gap of self-assembled films, we can conclude that there exist a strong correlation between the electronic structure and the geometrical structure of the ZnO arrays and the theoretical work is in progress.

The crystallinity of self-assembled film is poor compared to powder. Earlier observations have revealed that crystallinity of ZnO thin film was improved by annealing at high temperatures. Hence it is possible to develop other orientations by annealing at high temperatures and the mechanical properties of the self-assembled film can be improved after heat treatment. Although ZnO self-assembled films can act as photonic crystals, unfortunately, we are not able to observe photonic crystal properties and the work is in progress.

Typical results of the open aperture z-scan measurements which correspond to the far-field normalized transmittance as a function of the distance from the lens focus of the ZnO colloid and film for different particle sizes at an intensity of 220 MW/cm^2 for an irradiation wavelength of 532 nm are shown in Fig. 4a and b respectively. The open aperture curve exhibits a normalized transmittance valley, indicating the presence of reverse saturable absorption in the colloid and a transmittance peak, indicating the presence of saturable absorption in the self-assembled film. Reverse saturable absorption is characterized by decrease of transmittance with the increase of the energy input, whereas the opposite happens in SA. Here, we have to consider the transmittance of the sample under two situations: (1) in the presence of RSA and (2) in the presence of SA.

RSA is also referred to as induced absorption and there are various mechanisms leading to this process [12]. In the presence of RSA the optical nonlinearity is described by the equation

$$\alpha(I) = \alpha_0 + \beta I\,, \tag{1}$$

where α_0 is the linear absorption coefficient (cm^{-1}) and β is the nonlinear absorption cross section (mW^{-1}). The propagation through the sample is given by the relation

$$\frac{\mathrm{d}I}{\mathrm{d}z} = -\alpha(I)I\,. \tag{2}$$

Solving (2) by integrating between limits I_0 to I, and putting transmission $T = I/I_0$, we get

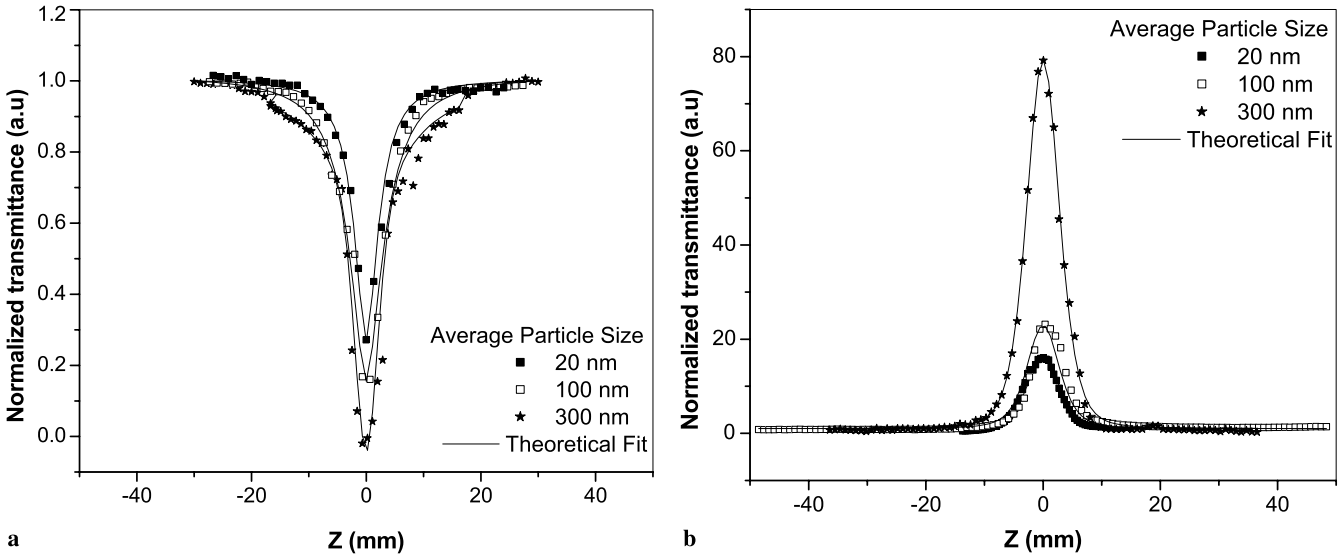

FIGURE 4 (**a**) Open aperture z-scan traces of ZnO colloids of different particle sizes at an intensity of 220 MW/cm^2 for an irradiation wavelength of 532 nm; (**b**) Open aperture z-scan traces of ZnO self-assembled films of different particle sizes at an intensity of 220 MW/cm^2 for an irradiation wavelength of 532 nm

$$T = \frac{\mathrm{e}^{-\alpha_0 L}}{1+\beta I_0 L_{\mathrm{eff}}}\,, \tag{3}$$

where

$$L_{\mathrm{eff}} = \frac{1-\mathrm{e}^{-\alpha_0 L}}{\alpha_0}\,, \tag{4}$$

where I_0 is the position dependent intensity. The position dependence in intensity should be incorporated into the expression by considering the variation of beam size on either side of the focus ($w(z)$). The equation is

$$w(z)^2 = w_0^2\left[1+\frac{z^2}{z_0^2}\right]\,, \tag{5}$$

where $z=0$ is the focus and $z_0 = \frac{\pi w_0^2}{\lambda}$ is referred to as the Rayleigh range or diffraction length of the beam and the nonlinear absorption coefficient β is obtained by fitting the experimental z-scan plot to (6).

$$T(z) = \frac{C}{q_0\sqrt{\pi}}\int_{-\infty}^{\infty}\ln\left(1+q_0\mathrm{e}^{-t^2}\right)\mathrm{d}t\,, \quad \text{where}$$
$$q_0(z,r,t) = \beta I_0 L_{\mathrm{eff}}\,. \tag{6}$$

The solid curve in Fig. 4a is the theoretical fit to the experimental data. From the value of β, we can calculate the imaginary part of susceptibility and β is related to Im $(\chi^{(3)})$ through the relation

$$\mathrm{Im}\,(\chi^{(3)}) = \frac{\lambda\varepsilon_0 n_0^2 c\beta}{4\pi}\,, \tag{7}$$

where λ is the excitation wavelength, $n_0 = 2.008$ is the linear refractive index of ZnO, ε_0 is the permittivity of free space and c the velocity of light in vacuum.

Now let us consider the beam propagation in a thin saturable absorber; the optical intensity loss is governed by the following differential equation:

$$\frac{\mathrm{d}I}{\mathrm{d}z} = -\alpha_{\mathrm{i}}(I)\,I\,, \tag{8}$$

where z and I are the propagation distance and the optical intensity inside the saturable absorption sample, respectively [21]. α_{i} is the intensity dependent absorption coefficient and is given by

$$\alpha_{\mathrm{i}}(I) = \frac{\alpha_0}{1+\left(\frac{I}{I_{\mathrm{S}}}\right)}\,, \tag{9}$$

where I_{S} is the saturation intensity. Substituting this in (8) and integrating between the limits I_0 to I_{L} gives

$$\ln\frac{I_{\mathrm{L}}}{I_0} = -\alpha_0 L - \left(\frac{I_L - I_0}{I_0}\right)\,. \tag{10}$$

This can be solved numerically to get the transmission of the sample, I_{L}. If excitation intensity I_0 is less than I_{S}, we can consider SA as a third-order process and in such cases $-\alpha_0/I_{\mathrm{S}}$ is equivalent to nonlinear absorption coefficient β, which will then give Im $(\chi^{(3)})$.

The enhanced nonlinear optical properties of ZnO colloids with increase in particle size are due to strong two photon absorption. The theory of two photon absorption process fitted well with the experimental curve and two photons of 532 nm radiation lie below the absorption band edge of the samples under investigation infers that TPA is the basic mechanism. When the crystallite size is reduced to the order of an exciton Bohr radius a_{B}, quantum size effects appear and drastic changes of optical properties are expected. The quantum confinement effects in semiconductor nanocrystals can be classified into two regimes, i.e., strong and weak confinement regimes, according to the ratio of nanocrystal radius R to

a_B [22]. Nonlinear optical properties in nanocrystals have also been investigated for the corresponding confinement regimes. In ZnO, the exciton Bohr radius is 2 nm, which is roughly 4 times that of CuCl, and one can investigate confinement effects and size dependence of $\chi^{(3)}$ over a wide range of crystallite sizes [23]. The susceptibility is size dependent, without showing a saturation behavior in the size range studied in our investigation. The enhancement of nonlinear optical properties with increasing dimension in the weak confinement regime essentially originates from the size dependent enhancement of oscillator strength of coherently generated excitons. Since the exciton is confined in a quantum dot, the confinement of excitonic wave function is expected to give rise to enhancement of the oscillator strength per quantum dot by a factor of R^3/a_B^3 [24]. This size dependent oscillator strength was experimentally confirmed in CuCl quantum dots. Such a giant oscillator strength effect will result in an enhancement of the nonlinear susceptibility [25].

The switching of saturable absorption behaviour in self-assembled ZnO from reverse saturable absorption in colloidal ZnO is shown in Fig. 4b for the same input energy and wavelength. Such an interesting effect can be used for optical pulse compression, optical switching and laser pulse narrowing [26]. The z-scan data shows that, along with moving the self-assembled film towards the focus, the increase in the laser intensity induces bleaching in the ground state absorption, which results in a transmittance increase (SA process).

The self-assembled film exhibits saturation of absorption and bleaching and possesses a larger absorption coefficient than colloid and, thereby, may have been even more susceptible to thermal effects. For semiconductor materials, heat tends to reduce the fermi energy level and thereby, increase the number of carriers in the conduction band. This, in turn, depletes the ground level and induces bleaching in the ground state absorption, which results in SA process. The origin of optical nonlinearity is not only dependent on polarization response of bound electrons leading to dielectric contributions but also from conduction electrons in semiconductors to which ZnO can be categorized. From Fig. 1, it is clear that the band gap of self-assembled film is reduced to 3.1 eV from that of bulk (3.3 eV) and the laser intensity induces bleaching in the ground state absorption, which results in SA process. But the band gap energies of the colloid is higher than that of the bulk which leads to induced absorption.

The sensitivity of ZnO to impurities as well as native defects with respect to electronic properties is well known [27]. The breadth of the absorption edge of the self assembly film indicates that there are defect-related transitons in this case. The negative β value in ZnO thin films were reported to be due to the saturated absorption of the defect states [27]. A similar explanation can hold for our self-assembled films also.

Figure 5 gives the closed aperture z-scan traces of ZnO colloid and self-assembled film at an intensity of 220 MW/cm^2 for an irradiation wavelength of 532 nm. The closed aperture curve exhibited a peak to valley shape, indicating a negative value of the nonlinear refractive index n_2. There is no change in the sign of nonlinear refractive index whereas the absorptive nonlinearity reverses its sign when the material changes from colloid to self-assembled film.

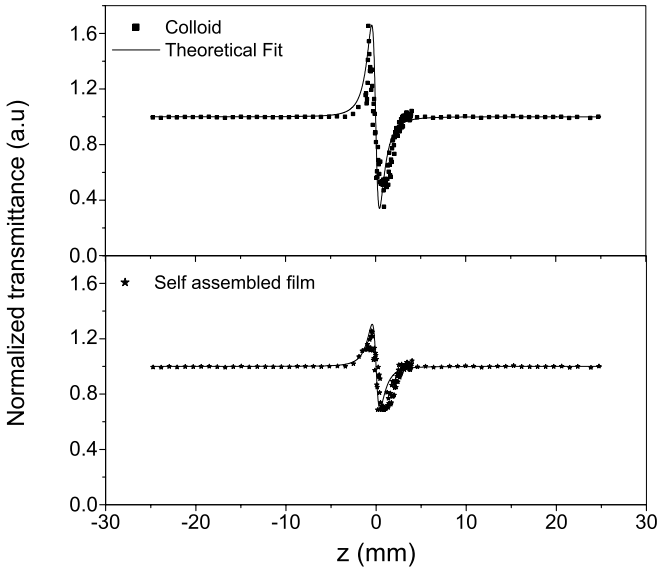

FIGURE 5 Closed aperture z-scan traces of ZnO colloid and self-assembled film of particle size 300 nm at an intensity of 220 MW/cm^2 for an irradiation wavelength of 532 nm

For samples with sizeable refractive and absorptive nonlinearities, closed aperture measurements contain contributions from both the intensity dependent changes in the transmission and in refractive index [15]. By dividing the normalized closed-aperture transmittance by the corresponding normalized open aperture data, we could retrieve the phase distortion created due to the change in refractive index and this result is depicted in Fig. 5.

It is observed that the peak–valley of closed aperture z-scan satisfied the condition $\Delta z \sim 1.7 z_0$, thus confirming the presence of cubic nonlinearity [15]. The value of ΔT_{p-v} i.e., the difference between the peak and valley transmittance could be obtained by the best theoretical fit from the results of divided z-scan curve. The nonlinear refractive index n_2 and the real part of nonlinear susceptibility Re $\chi^{(3)}$ are given, respectively, by

$$n_2(\text{esu}) = \frac{Cn_0}{40\pi^2}\frac{\lambda\Delta T_{p-v}}{0.812(1-S)^{0.25}L_{\text{eff}}I_0} \quad \text{and}$$
$$\text{Re}\,(\chi^{(3)})(\text{esu}) = \frac{n_0 n_2(\text{esu})}{3\pi}\,. \tag{11}$$

The nonlinear absorption coefficient, refractive index and third-order susceptibility of ZnO colloid and self-assembled film of particle size 300 nm at an intensity of 220 MW/cm^2 and at a wavelength of 532 nm are tabulated in Table 1. When it is a saturable absorber, a more useful parameter to extract from the transmission measurements is the saturation intensity I_S, which is also given in the table. It can also be assumed that for a saturable absorber $-\alpha_0/I_S$ is equivalent to β of a RSA material. Henari et al. used the same technique to find out the nonlinear optical parameters of group IV metal phthalocyanines using 665 nm, picosecond laser [28]. The absolute values of β and I_S values obtained by them are at least one order of magnitude higher than what we observed. We attribute these differences to the type of laser excitation and to the differences in the sample properties.

	$\beta \times 10^{-8}$ m/W	I_S GW/cm^2	n_2 esu	Im $(\chi^{(3)})$ esu	Re $(\chi^{(3)})$ esu	$\chi^{(3)}$ esu
Colloid	1.17	–	-4.3×10^{-9}	5.1×10^{-10}	-9.2×10^{-10}	10.5×10^{-10}
Self assembled film	–	0.40	-2.8×10^{-5}	-0.6×10^{-6}	-5.9×10^{-6}	5.93×10^{-6}

TABLE 1 Measured values of nonlinear absorption coefficient, saturation intensity, refractive index and third-order susceptibility of ZnO colloid and self-assembled film of particle size 300 nm at an intensity of 220 MW/cm^2 for an irradiation wavelength of 532 nm

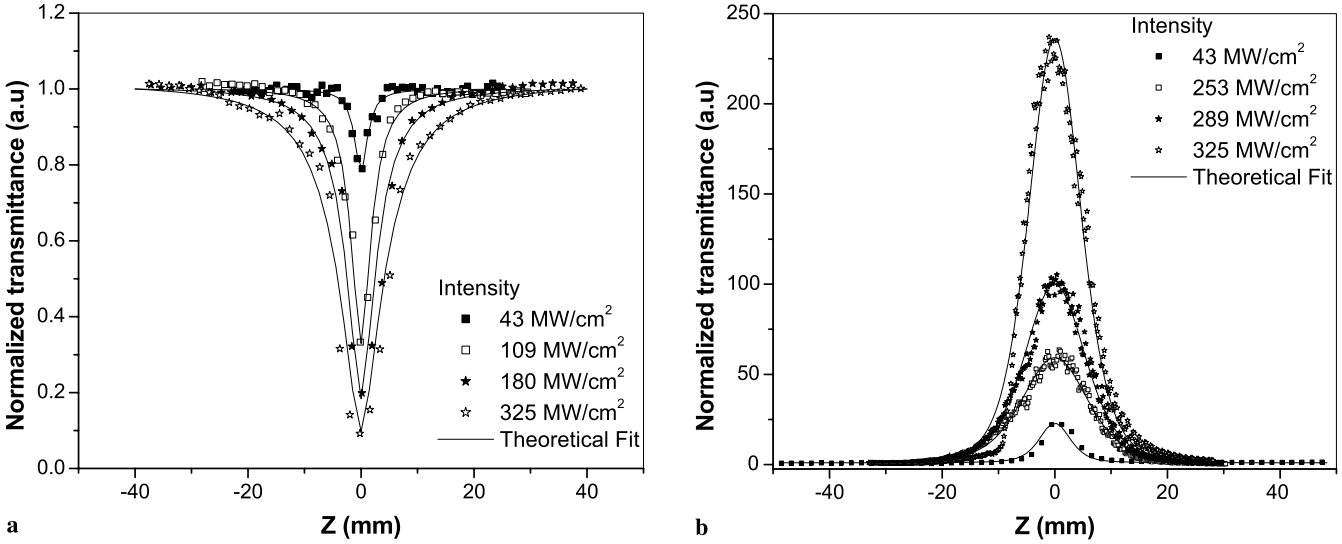

FIGURE 6 (**a**) Open aperture z-scan curves of ZnO colloid of size 300 nm at a wavelength of 532 nm for different input intensities; (**b**) Open aperture z-scan curves of ZnO self-assembled films of size 300 nm at a wavelength of 532 nm for different input intensities

In general, induced absorption can occur due to a variety of processes. However, the dominant mechanism is decided by factors such as duration of the excitation pulse, lifetimes of excited singlet and triplet states and intersystem crossing time, crossing yield, etc. Nonlinear absorption can occur by instantaneous two photon absorption (TPA) or through sequential TPA. This is an irradiance dependent process [29]. If the molecules undergo vibrational relaxation and then reaches excited state by further absorption, it is referred to as the singlet excited state absorption (ESA). Unlike TPA, ESA is a fluence dependent process. This means that the same fluence for two different pulse widths will give the same nonlinear absorption if the mechanism is ESA. By measuring the nonlinear absorption for various pulse durations, it is possible to confirm whether ESA or TPA dominates in contributing to induced absorption. As a rule, transmittance change ΔT at a fixed pulse energy will be independent of pulse width if the mechanism is ESA but will depend on pulse width if it is TPA.

The open aperture z-scan curves of ZnO colloid and self-assembled film of size 300 nm at a wavelength of 532 nm for different input intensities is shown in Fig. 6a and b respectively. We can see that nonlinear optical properties are highly irradiance dependent. The colloid shows reverse saturable absorption at all intensities under investigation. The results show three orders of enhancement from the reported value of 5 cm/GW for bulk ZnO [30]. It has been reported that the reduced dimensionality of the particles resulted in considerable enhancement of the second-order susceptibility $\chi^{(2)}$ in thin films of ZnO [31]. Similar results in the third-order nonlinear parameters are evident in our measurements also. The dependence of nonlinear absorption with input intensity

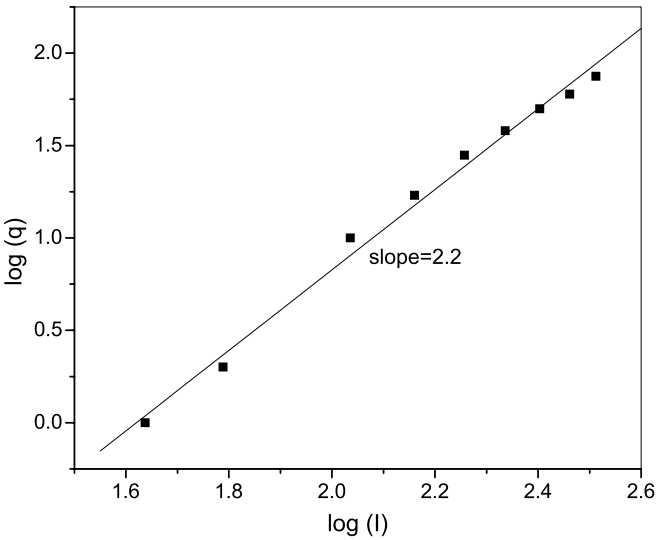

FIGURE 7 Variation of $\log q$ as a function of $\log I$ for ZnO colloid of size 300 nm at a wavelength of 532 nm. Slope of the plot gives 2.2, which suggests that the dominant mechanism contributing to induced absorption is TPA

is due to TPA as clearly seen from $\log q$ vs. $\log I$ plot shown in Fig. 7. The parameter q is the depth of the open aperture z-scan curve obtained from the theoretical fit and is a measure of intensity dependent absorption and I is the irradiance at focus. Slope of the plot in Fig. 7 gives 2.2, which infers that TPA is the basic mechanism and there is the possibility of higher order nonlinear processes such as free carrier absorption (FCA) contributing to induced absorption. The free carrier life time of ZnO is reported to be 2.8 ns [32]. Hence

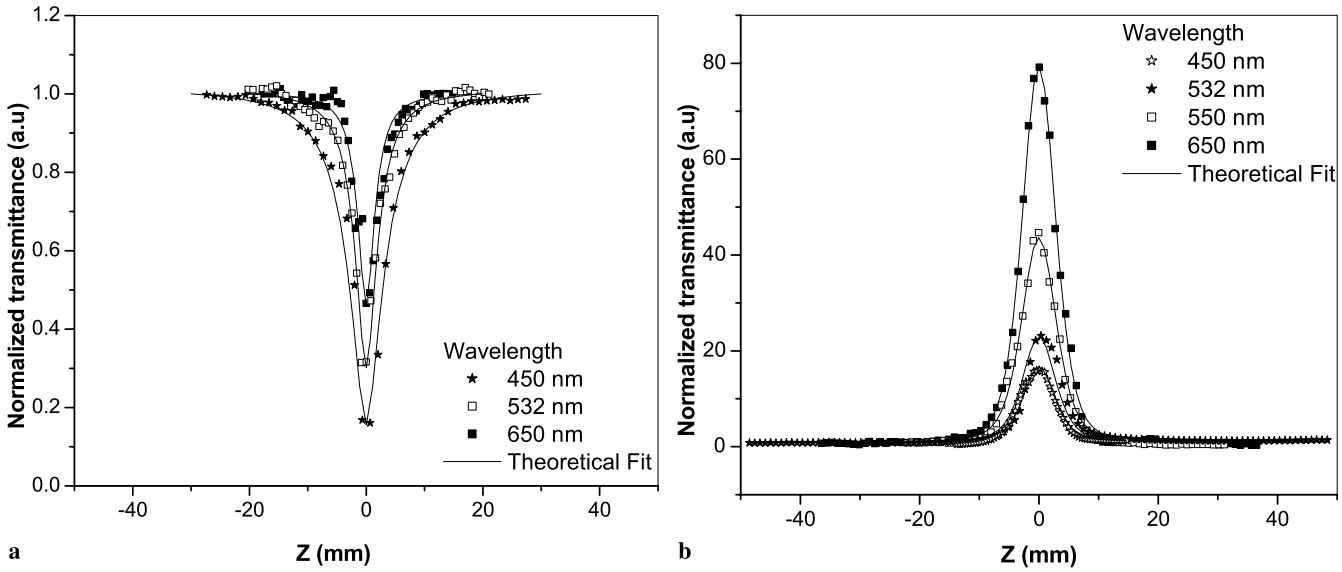

FIGURE 8 (**a**) Open aperture z-scan curves of ZnO colloid of size 300 nm at an intensity of 220 MW/cm^2 for different wavelengths; (**b**) Open aperture z-scan curves of ZnO self-assembled films of size 300 nm at an intensity of 220 MW/cm^2 for different wavelengths

there is a strong possibility that the 7 ns pulses used in the present study is exciting the accumulated free carriers generated by TPA by the rising edge of the pulse. Considering all these factors and also that we used nanosecond excitation pulses, it is reasonable to assume that TPA and FCA are the important mechanisms contributing to induced absorption in our samples.

Now we will evaluate the saturable intensity of the self-assembled film and attempt to interpret its SA behavior. We use the SA model described in (9) to fit our experimental OA z-scan trace displayed in Fig. 6b, with only one adjustable parameter (I_S) and the model is in good arrangement with the experimental data. The theoretical fitting give the respective I_S to be within a range of 0.12–0.52 GW/cm^2, for different intensity levels of I_0 ranging from 40 to 325 MW/cm^2, respectively. The results imply certainly that the self-assembled films show SA behavior and no reverse saturable absorption phenomena are observed. It is well known that the theoretical model could describe the SA effect in a homogeneous broadening two level system very well. In the self-assembled film, the strong SA and the absence of RSA implies that the absorption cross-section of ground state is much larger than the absorption cross-section of excited state.

We have observed that the nature of nonlinear absorption in ZnO is dependent on the wavelength of the excitation beam. It is seen that the material exhibits RSA for all wavelengths under investigation when it is in colloidal form. The self-assembled film exhibits SA and the material does not exhibit any sign of absorptive nonlinearity for all wavelengths under investigation. This interesting feature is illustrated in Fig. 8a and b. However, it can be concluded that the nonlinear absorption changes from RSA to SA when the material changes from colloidal form to self-assembled film.

All RSA materials possess a higher absorption cross-section of excited states (σ_e) compared to that of the ground state (σ_g) at the excitation radiation wavelength [33]. Interestingly they will also give a positive value for the imaginary part

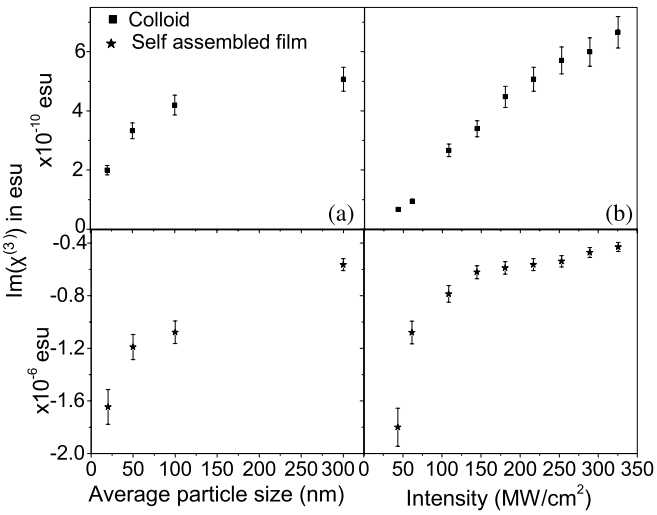

FIGURE 9 Variation of imaginary part of susceptibility with (**a**) particle size; (**b**) Intensity

of susceptibility Im ($\chi^{(3)}$) which is actually a measure of the induced absorption. On the other hand, a saturable absorber has a negative value for Im ($\chi^{(3)}$).

The calculated values of Im ($\chi^{(3)}$) as a function of size and intensity are shown in Fig. 9a and b respectively and it is found that susceptibility increases with particle size and intensity. $\chi^{(2)}$ and $\chi^{(4)}$ vanish in liquids and higher order odd terms such as $\chi^{(5)}$ will be very small compared to $\chi^{(3)}$. These values are within an error of 7% contributed mainly by the uncertainty in intensity measurements in the sample and the fitting error. One should be very careful while comparing the susceptibility values available in literature. These values vary to a great extent depending on the excitation wavelength, pulse duration, experimental technique, concentration of the molecular species in the sample etc. It is worth noting that certain representative third-order nonlinear optical materials, such as CuO chain compounds, Ag_2S/CdS nanocom-

posites, metallophthalocyanines, porphrins, organic dyes, organic polymers, organic coated quantum dots, metal clusters etc., yielded values of order of 10^{-10} to 10^{-14} esu for $\chi^{(3)}$ at a wavelength of 532 nm [34–37]. These values are comparable to the value of $\chi^{(3)}$ obtained for colloids in the present investigation. The values of $\chi^{(3)}$ measured at room temperature by femtosecond degenerate four wave mixing technique on ZnO microcrystalline thin films grown by laser molecular beam epitaxy on sapphire substrate are of the order of 10^{-5} to 10^{-8} esu and are comparable with the values obtained for self-assembled films in the present investigation [38]. The enhancement of $\chi^{(3)}$ for thin nanocrystalline films compared to microcrystalline films of ZnO was attributed to the nanosized structure of the film [39]. Thus, the real and imaginary parts of third-order nonlinear optical susceptibility measured by the z-scan technique revealed that the ZnO colloids and self-assembled films investigated in the present study have good nonlinear optical response and could be chosen as ideal candidates with potential applications for nonlinear optics.

The calculated values of Im $(\chi^{(3)})$ as a function of wavelength are shown in Fig. 10a. It will be useful to define a figure of merit (FOM) for these types of materials as the ratio Im $(\chi^{(3)})/\alpha_0$, which specifies the magnitude of nonlinear absorption for unit value of linear absorption loss. FOM as a function of wavelength is plotted in Fig. 10b and it is found that FOM is larger in the region between 450 and 550 nm. It helps in comparing the absorptive nonlinearities at various excitation wavelengths.

The most important application of these materials is in optical limiting and to be used as a saturable absorber. Since these properties are spectral dependent, it is more common to use another figure of merit, σ_e/σ_g, which is the ratio of excited to ground state absorption cross-section. The value of σ_g can be obtained from the linear absorption spectrum using Beer's law. To evaluate σ_e we need to analyze the z-scan signal in a manner, as suggested by Wei et al. [29]. These features are under investigation and will be communicated later.

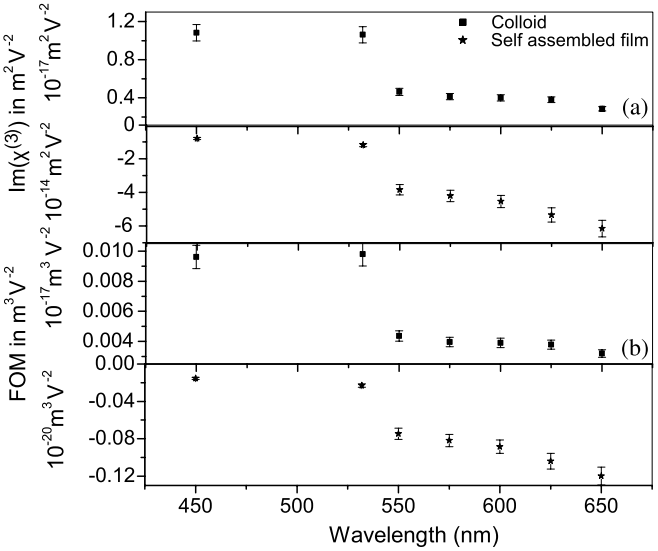

FIGURE 10 (**a**) Imaginary part of susceptibility as a function of wavelength; (**b**) Figure of merit as a function of wavelength

4 Conclusion

The nonlinear optical properties of self-assembled films formed from ZnO colloidal spheres have been investigated by z-scan technique. The sign of the nonlinear component of refractive index of the material remains the same; however a switching from reverse saturable absorption to saturable absorption has been observed as the material changes from colloid to self-assembled films. These different nonlinear characteristics can be mainly attributed to ZnO defect states and electronic effects when the colloidal solution is transformed into self-assembled monolayers. In the self-assembled film, the strong SA and the absence of RSA implies that the absorption cross-section of ground state is much larger than the absorption cross section of excited state. We report our investigations of intensity, wavelength and size dependence of saturable and reverse saturable absorption of ZnO self-assembled films and colloids. Values of the imaginary part of third-order susceptibility are calculated for particles of size in the range 20–300 nm at different intensity levels ranging from 40 to 325 MW/cm^2 within the wavelength range of 450–650 nm. The wavelength dependence of figure of merit is calculated, which helps in comparing the absorptive nonlinearities at various excitation wavelengths.

ACKNOWLEDGEMENTS L.I. acknowledges UGC for research fellowship. B.K. wishes to acknowledge C-MET for the support and permission given to pursue this work.

REFERENCES

1 O. Painter, R.K. Lee, A. Scherer, A. Yariv, J.D. O'Brien, P.D. Dapkus, I. Kim, Science **284**, 1819 (1999)
2 H.B. Sun, S. Matsuo, H. Misawa, Appl. Phys. Lett. **74**, 786 (1999)
3 E.W. Seelig, B. Tang, A. Yamilov, H. Cao, R.P.H. Chang, Mater. Chem. Phys. **9712**, 1 (2002)
4 S.H. Park, Y.N. Xia, Langmuir **15**, 266 (1999)
5 S.G. Romanov, T. Maka, C.M.S. Torres, M. Muller, R. Zentel, Appl. Phys. Lett. **79**, 731 (2001)
6 K.P. Velikov, A. van Blaaderen, Langmuir **17**, 4779 (2001)
7 H. Cao, J.Y. Xu, D.Z. Zhang, S.H. Chang, S.T. Ho, E.W. Seelig, X. Liu, R.P.H. Chang, Phys. Rev. Lett. **84**, 5584 (2000)
8 N. Fujimura, T. Nishihara, S. Goto, J. Xu, T. Ito, J. Cryst. Growth **130**, 269 (1993)
9 L. Vayssieres, K. Keis, S.-E. Lindquist, A. Hagfeldt, J. Phys. Chem. B **105**, 3350 (2001)
10 R.L. Sutherland, *Handbook of Nonlinear Optics* (Marcel Dekker, New York, 1996), Chapt. 9
11 Y.X. Fan, J.L. He, Y.G. Wang, S. Liu, H.T. Wang, X.Y. Ma, Appl. Phys. Lett. **86**, 101 103 (2005)
12 M.S. Bahae, A.A. Said, T.H. Wei, D.J. Hagan, E.W. Van Stryland, IEEE J. Quantum Electron. **QE-26**, 760 (1990)
13 B. Gu, J. Wang, J. Chen, Y.X. Fan, J.P. Ding, H.T. Wang, Opt. Express **13**, 9230 (2005)
14 J. He, W. Ji, G.H. Ma, S.H. Tang, H.I. Elim, W.X. Sun, Z.H. Zhang, W.S. Chin, J. Appl. Phys. **95**, 6381 (2004)
15 M.S. Bahae, A.A. Said, E.W. van Stryland, Opt. Lett. **14**, 955 (1989)
16 D.L. Moreno, E.D. Rosa-Cruz, F.J. Cuevas, L.E. Regalado, P. Salas, R. Rodriguez, V.M. Castano, Opt. Mater. **19**, 275 (2002)
17 S. Sapra, D.D. Sarma, Phys. Rev. B **69**, 125 304 (2004)
18 L. Guo, S. Yang, C. Yang, P. Yu, J. Wang, W. Ge, G.K.L. Wong, Appl. Phys. Lett. **76**, 2901 (2000)
19 J.G.E. Gardeniers, Z.M. Rittersm, G.J. Burger, J. Appl. Phys. **83**, 7844 (1998)
20 A. Kuroyanagi, Japan. J. Appl. Phys. **28**, 219 (1989)
21 R. Rojo, S. Yamada, H. Matsuda, J. Opt. Soc. Am. B **15**, 2937 (1998)
22 L.E. Brus, J. Chem. Phys. **80**, 4403 (1984)
23 H.L. Cao, X.F. Qian, Q. Gong, W.M. Du, X.D. Ma, Z.K. Zhu, Nanotechnology **17**, 3632 (2006)

24 E. Hanamura, Phys. Rev. B **37**, 1273 (1988)
25 A. Nakamura, H. Yamada, T. Tokizaki, Phys. Rev. B **40**, 8585 (1989)
26 Y.B. Band, D.J. Harter, R. Bavli, Chem. Phys. Lett. **126**, 280 (1986)
27 J.-H. Lin, Y.-J. Chen, H.-Y. Lin, W.-F. Hsieh, J. Appl. Phys. **97**, 033 526 (2005)
28 F.Z. Henari, J. Callaghan, W.J. Blau, P. Haisch, M. Hanack, Pure Appl. Opt. **6**, 741 (1997)
29 T.H. Wei, D.J. Hagan, M.J. Sence, E.W. Stryland, J.W. Perry, D.R. Coulter, Appl. Phys. B **54**, 46 (1992)
30 M.J. Weber (Ed.), *CRC Handbook of Laser Science and Technology: Optical Materials* (CRC Press, Boca Raton, 1997)
31 G. Wang, G.T. Kiehne, G.K.L. Wong, J.B. Ketterson, X. Liu, R.P.H. Chang, Appl. Phys. Lett. **80**, 401 (2002)
32 X.J. Zhang, W. Ji, S.H. Tang, J. Opt. Soc. Am. B **14**, 1951 (1997)
33 P.J. Gonalves, I.E. Borissevitch, L. de Boni, N.M. Barbosa Neto, J.J. Rodrigues Jr., S.C. Zlio, XXVI Encontro Nacional de Física da Matétia Condensada, 2003 Caxambu. XXVI ENFMC-Annals of Optics, Vol. **V5** (2003)
34 H.P. Li, B. Liu, C.H. Kam, Y.L. Lam, W.X. Que, L.M. Gan, C.H. Chew, G.Q. Xu, Opt. Mater. **14**, 321 (2000)
35 S. Shi, W. Ji, S.H. Tang, J. Am. Chem. Soc. **116**, 3615 (1994)
36 A. Maeda, M. Ono, H. Kishida, T. Manako, A. Sawa, M. Kawasaki, Y. Tokura, H. Okamoto, Phys. Rev. B **70**, 125 117 (2004)
37 M.Y. Han, W. Huang, C.H. Chew, L.M. Gan, X.J. Zhang, W. Ji, J. Phys. Chem. B **102**, 1884 (1998)
38 W. Zhang, H. Wang, K.S. Wong, Z.K. Tang, G.K.L. Wong, J. Ravinder, Appl. Phys. Lett. **75**, 3321 (1999)
39 R. Adair, L.L. Chase, S.A. Payne, Phys. Rev. B **39**, 3337 (1989)